Thermally induced delamination of amorphous hydrogenated carbon coatings monitored by positron beam analysis

Escobar Galindo, R.; Veen, A. van; Schut, H.; Rabbani, F.; Janssen, G.C.A.M.; Hosson, J.Th.M. De

Published in:
Surface & Coatings Technology

DOI:
10.1016/S0257-8972(03)01190-3

Publication date:
2004

Available online at www.sciencedirect.com
SCIENCE DIRECT®
Surface and Coatings Technology 180–181 (2004) 207–212
SURFACE & COATINGS TECHNOLOGY
www.elsevier.com/locate/surfcoat

Thermally induced delamination of amorphous hydrogenated carbon coatings monitored by positron beam analysis

R. Escobar Galindo[a,*], A. van Veen[a], H. Schut[a], F. Rabbani[b], G.C.A.M. Janssen[b], J.Th.M. De Hosson[c]

[a]*Defects in Materials, Interfaculty Reactor Institute, Delft University of Technology, Mekelweg 15, NL-2629 JB Delft, The Netherlands*
[b]*Department of Materials Science and Technology, Delft University of Technology, Rotterdamseweg 137, NL-2628 AL Delft, The Netherlands*
[c]*Materials Science Centre and NIMR, University of Groningen, Nijenborgh 4, NL-9747 AG Groningen, The Netherlands*

Abstract

In this work we have studied the adhesion of PVD amorphous hydrogenated carbon (a-C:H) thin coatings (<200 nm) on crystalline silicon by means of positron beam analysis (PBA). PBA allows the study of the a-C:H layer and the interface by monitoring changes on the Doppler broadening parameters *S* and *W*. Depending on the deposition condition, using PBA some samples were found to be delaminated after deposition. Annealing experiments were performed on samples that did not show signs of delamination after deposition. Some of these samples were distinguished by the fact that nitrogen was used in the manufacturing process. Samples were annealed for 30 min in vacuum up to 600 °C in order to remove gases absorbed at the interface. PBA experiments were performed after each annealing step. For the sample without N_2 there are no *S*–*W* changes either in the coating or at the interface until 600 °C is reached. On the other hand, for the sample containing N_2, there is a gradual change in these parameters with temperature. In this coating, after annealing to 500 °C, the increase in *W* is related to release of H_2 and consequent restructuring of the layer. The decrease in the value of *S* between 500 and 600 °C indicates the formation of graphitic crystallites. There is open volume at the coating/substrate interface since the *S* parameter gradually increases while *W* remains constant until 400 °C. This behaviour in *S*–*W* is related to the removal of physisorbed hydrogen. At approximately 400 °C the H bonded to C at tetrahedral sites is also released which leads to an internal restructuring of the 'lattice', hence a decrease in the value of *S* is observed. Finally, at 600 °C both coatings delaminate, as the interface parameters tend towards the same values as those of the sample which had delaminated after deposition.

Keywords: Positron beam analysis; Doppler broadening; Annealing; a-c:H; Delamination

1. Introduction

Diamond-like carbon (DLC) coatings are of great interest in a wide range of industrial applications because of their low coefficient of friction, good wear rate, high hardness, optical transparency, low surface energy, chemical inertness and biocompatibility [1]. These films have been used as protective coatings in microelectronics devices [2–4], in optics as commercially available scratch resistant materials for use in laser barcode scanners [5], in magnetic and magneto-optic recording disks [6], in tribological applications such as self lubricating bearings and metal forming tools and in biomedicine [7] [8]. The diamond-like properties of the DLC films are mainly determined by the sp^3/sp^2 ratio and the hydrogen content. In a recent work Robertson [9] reviews in great detail the deposition and characterisation methods, electronic structure, defects, mechanical properties and applications of diamond-like-amorphous carbon films. The different forms of amorphous carbon are also described, including amorphous hydrogenated carbon (a-C:H) coatings, the subject of this study.

One of the main concerns in the applications of DLC coatings is the high compressive stress developed by the films during manufacture. In many cases this results in the failure of the coating by delamination or buckling [10]. Nitrogen incorporation in a-C:H has proven to be an effective way of reducing the internal stresses of the films without noticeably changing the hardness [11–14]. One of the reasons adduced for stress reduction is the increase in the density of voids in the films.

*Corresponding author. Tel.: +31-15-278-1612; fax: +31-15-278-6422.
E-mail address: rescobar@iri.tudelft.nl (R. Escobar Galindo).

0257-8972/04/$ - see front matter © 2003 Elsevier B.V. All rights reserved.
doi:10.1016/j.surfcoat.2003.10.042

Table 1
Description of the deposition conditions used to manufacture the amorphous carbon coatings and resultant film thickness

Sample	CH_4 (sccm)	Ar (sccm)	N_2 (sccm)	H_2 (sccm)	Bias (V)	Temperature (°C)	Thickness (nm)
1	50	0	0	50	550	270	135
2	50	0	20	50	550	270	90
3	100	80	20	100	600	~300	200
4	50	90	10	50	400	~300	125

Positron beam analysis (PBA) is a non-destructive technique particularly sensitive to the presence of open volume defects or voids [15]. This technique has been successfully applied to the study of different types of DLC films [11,16–18]. In this work we apply PBA to study the changes observed in the coatings and at the interface of a-C:H films as a result of annealing treatment. These results will be compared to Raman experiments performed on the same samples and presented in Ref. [19].

2. Experimental

Four different amorphous hydrogenated carbon coatings (a-C:H) were produced by a non-conventional process [19]. A Hauzer PVD machine was used to generate a reactive glow made from the decomposition of a range of gases with and without N_2, with CH_4 as the carbon containing gas. A description of the deposition conditions is given in Table 1. A DC-bias voltage of 550 V was applied to the substrate table and the gases were introduced at specific flow rates high enough to generate plasma. Two control samples (1 and 2 in Table 1) were made with temperature regulation i.e. the deposition was started at 270 °C and this temperature was maintained during the test by applying external heating not generated by the plasma. The deposition conditions and the gas mixture are identical for both samples except for the nitrogen content. The coatings were deposited onto Si $\langle 1\,0\,0 \rangle$ single crystal substrates, for a deposition time of 1 h. Prior to the coating procedure an etch step was included using Ar gas to remove the surface oxide layer on the Si substrate.

After deposition the samples were annealed for 30 min under a vacuum of approximately 10^{-5} Pa in order to remove gases absorbed at the interface. The annealing temperatures were: 150, 300, 400, 500 and 600 °C. PBA was used to analyse the coatings between each annealing experiment.

The PBA experiments were performed with the Delft variable energy positron beam (VEP) [20]. The positrons were injected into the samples with energies tuned between 100 and 30 keV. The maximum implantation energy corresponds to a typical implantation depth of ~ 4 μm for materials with a density of $\rho \sim 3$ g cm^{-3}. All experiments were carried out at room temperature (RT) under a vacuum of approximately 10^{-6} Pa. PBA results are described in terms of two parameters (S and W) related to the Doppler broadening of the 511 keV annihilation photo-peak. The S parameter indicates the fraction of positrons that annihilates with low momentum electrons (valence or conduction electrons). This parameter is related to the open volume defects present in the sample (e.g. pores). The W parameter indicates the fraction of positrons that annihilates with high momentum electrons (core electrons). This parameter is related to the chemical environment where the annihilation takes place. Both parameters can be combined in S–W maps with a third variable (i.e. implantation energy, annealing temperature or strain) as a running parameter. The different positron annihilation sites (layers) can then be distinguished. The data was analysed with the VEPFIT [21] program.

3. Results and discussion

3.1. PBA on as deposited amorphous carbon coatings

In Fig. 1 the PBA experimental results on the as received samples are presented. The samples were described in terms of 4 layers each of them ascribed to different positron annihilation sites: (1) surface, (2) a-C:H coating, (3) coating-substrate interface and (4) silicon substrate. These sites will hereafter be referred to as cluster points (CPs). The results summarised in Table 2 show that the control samples 1 and 2 have constant values of S and W for the coating layer. The S parameter is similar for both samples but the W parameter is higher for the coating with nitrogen (sample 2). This difference in W is related to annihilation in the vicinity of nitrogen as reported to occur for thin Zirconia layers with argon [22]. The presence of the interface (CP3) is clearly observed for both samples in Fig. 1b from the turn of the S–W values after the coating layer (CP2) towards the silicon substrate (CP4). The S value characterising the interface of sample 2 is higher than sample 1 without N_2 indicating a more porous structure at the interface of the first sample. Sample 3, although deposited under different conditions than the control samples 1 and 2, has similar positron results. On the other hand, sample 4 shows a completely different S–W map compared to the other three as deposited samples.

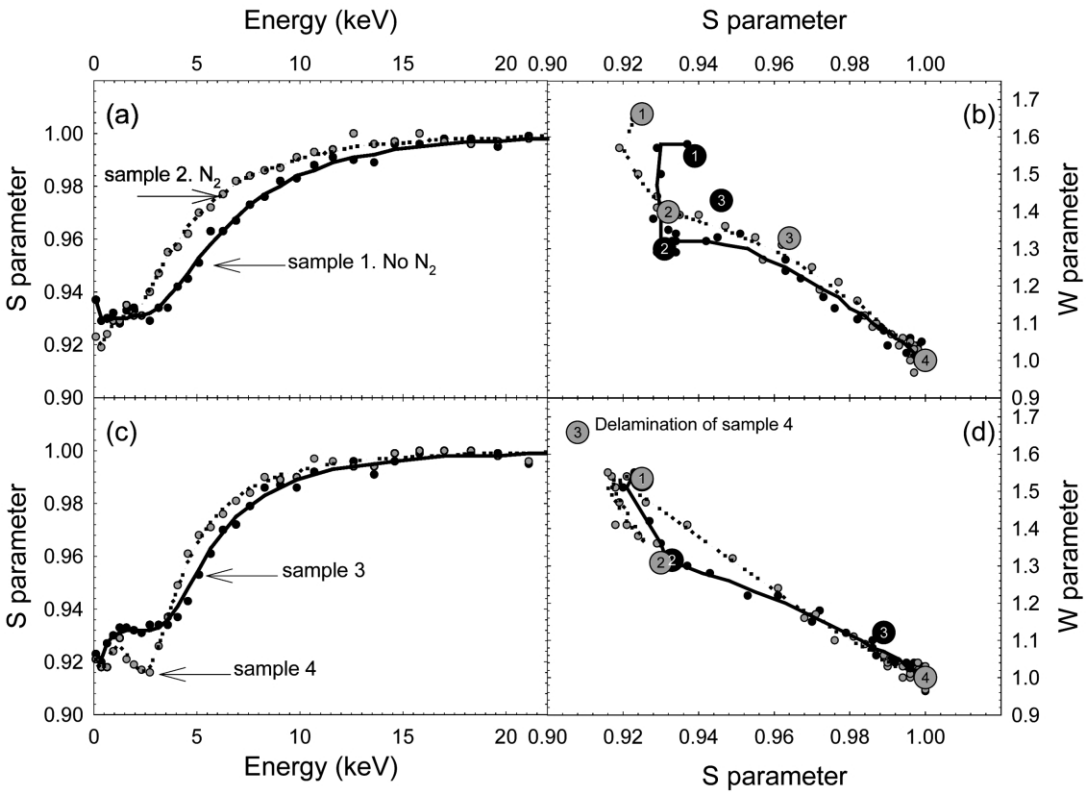

Fig. 1. Doppler broadening results on amorphous carbon films. The *S* parameter is plotted as a function of the positron implantation energy for (a) samples 1 and 2 and (c) samples 3 and 4 as deposited on silicon. The *S*–*W* maps are shown for (b) 1 and 2 and (d) 3 and 4 as deposited samples, respectively. The lines represent the VEPFIT analysis results. The numbered circles indicate the positron annihilation sites ascribed to 1—Surface; 2—Coating layer; 3—Interface and 4—Substrate.

In Fig. 1c, the *S* parameter of sample 4 first increases to a value similar to the other samples but, instead of further increasing towards the *S* value of the silicon substrate, it drops to a value close to the surface. In the *S*–*W* map of Fig. 1d this change is clearly observed as the *S*–*W* data after reaching the coating cluster point (CP2) looped back in the direction of the surface to a cluster point (CP3) with a low *S* and high *W*. It is interesting to notice that after this CP the *S*–*W* data lie on a straight line towards the silicon substrate CP. We ascribed this different behaviour to delamination of the coating as we will explain it later in the next section.

3.2. PBA on annealed amorphous carbon coatings

Annealing experiments were performed on samples 1, 2 and 3, coatings without signs of delamination after deposition. Samples were annealed for 30 min in vacuum up to a maximum temperature of 600 °C. PBA experiments were performed after each annealing step. In Fig. 2, we can observe the PBA results for the three annealed samples after the last annealing step as compared with the results for as deposited sample 4. The most remarkable observation is that the interface cluster point (CP3) for the three annealed samples is located at

Table 2
VEPFIT results on amorphous carbon samples, studied at RT (before delamination) and after 600 °C annealing (after delamination)

No.	Before annealing						After annealing			
	S_{coat}	W_{coat}	S_{delam}	W_{delam}	S_{interf}	W_{interf}	S_{coat}	W_{coat}	S_{delam}	W_{delam}
1	0.931	1.299	–	–	0.946	1.429	0.919	1.536	0.907	1.666
2	0.932	1.398	–	–	0.964	1.328	0.929	1.481	0.906	1.675
3	0.933	1.315	–	–	0.989	1.121	0.918	1.572	0.906	1.637
4	0.930	1.308	0.908	1.658	–	–	–	–	–	–

The absolute errors in *S* and *W* are $\Delta S \sim 0.002$ and $\Delta W \sim 0.03$, respectively.

the same position as for as deposited delaminated sample 4 (see S–W maps in Fig. 2b and d). With increasing positron implantation energy the S–W data lie on a straight line towards the CP of the silicon substrate. The process can be schematically described in Fig. 3. Before delamination occurs we have a closed interface (3) between the coating and the substrate. This results in a typical S–W map as observed in Fig. 1b with a loop between CP2 and CP4 indicating the presence of the interface (CP3). Once delamination occurs there is no longer a close interface and positrons annihilate in the new internal surfaces created (1* and 4* in Fig. 3). CP3 is now ascribed to positron annihilation in these new surfaces. This is the reason the S–W curves for samples annealed to 600 °C, and as deposited sample 4, turn back towards surface values (Fig. 2b and d). After that the S–W curves map a straight line to the substrate, as a free-standing sample would, with only two positron annihilation sites: surface and bulk.

The control samples 1 and 2 were manufactured to allow for the study of the role of nitrogen in the performance of the coatings during annealing. In Fig. 4, we follow the changes in S–W values with temperature, inside the coating (Fig. 4a), and at the interface (Fig. 4b). In Fig. 5, the S parameter for the interface is plotted as a function of annealing temperature. The sample without N_2 (sample 1) shows no significant change in the values of S–W either in the coating or at the interface until 600 °C is reached. As mentioned before, at this temperature there is a dramatic change in the interface

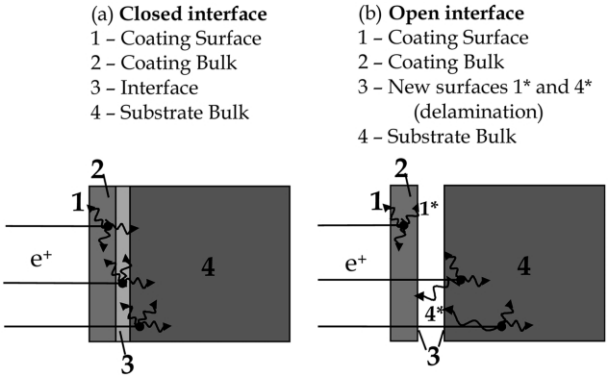

Fig. 3. Schematic representing the different positron annihilation sites for a coating/substrate system with (a) a closed interface and (b) with an open interface (delamination). In (b) the positron parameters of site 3 are an average of the positron parameters of the two new surfaces (1* and 4*) created after delamination. The schematic is not to scale.

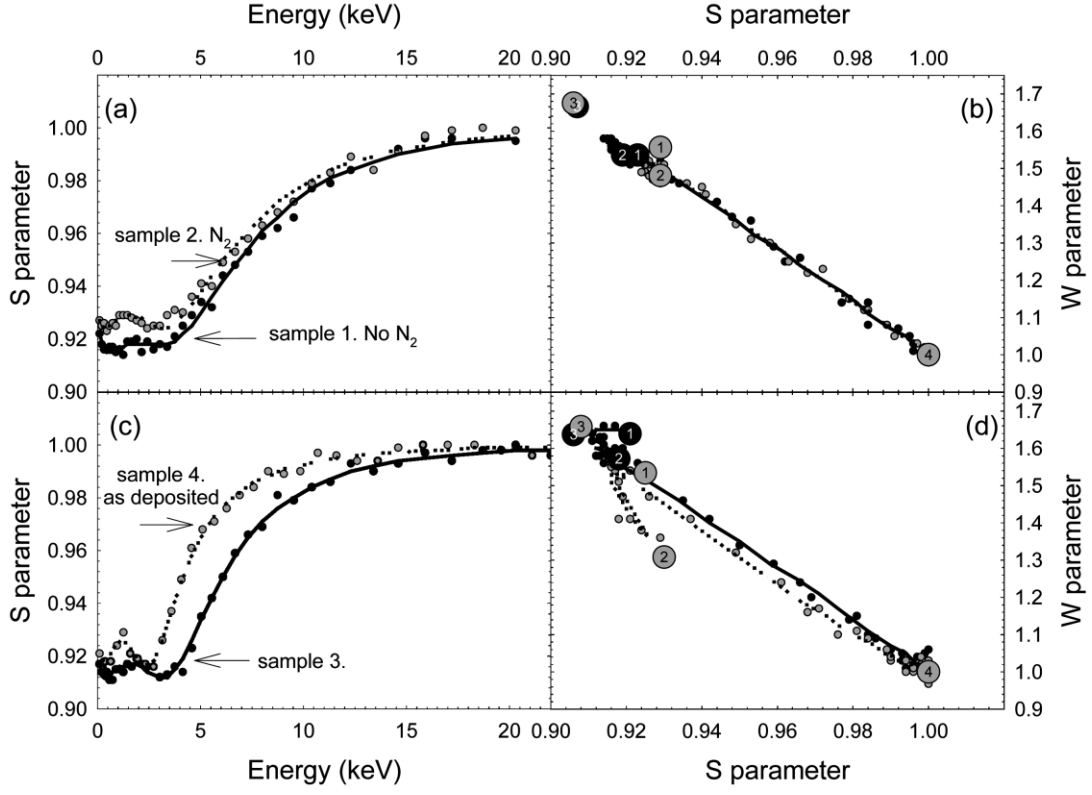

Fig. 2. Doppler broadening results on amorphous carbon films. The S parameter is plotted as a function of the positron implantation energy for (a) samples 1 and 2 after 600 °C annealing and (c) samples 3 after 600 °C annealing and 4 as deposited. The corresponding S–W maps are shown for (b) samples 1 and 2 and (d) samples 3 and 4, respectively. The lines represent the VEPFIT analysis results. The numbered circles indicate the positron annihilation sites ascribed to (1) surface; (2) coating layer; (3) interface and (4) substrate.

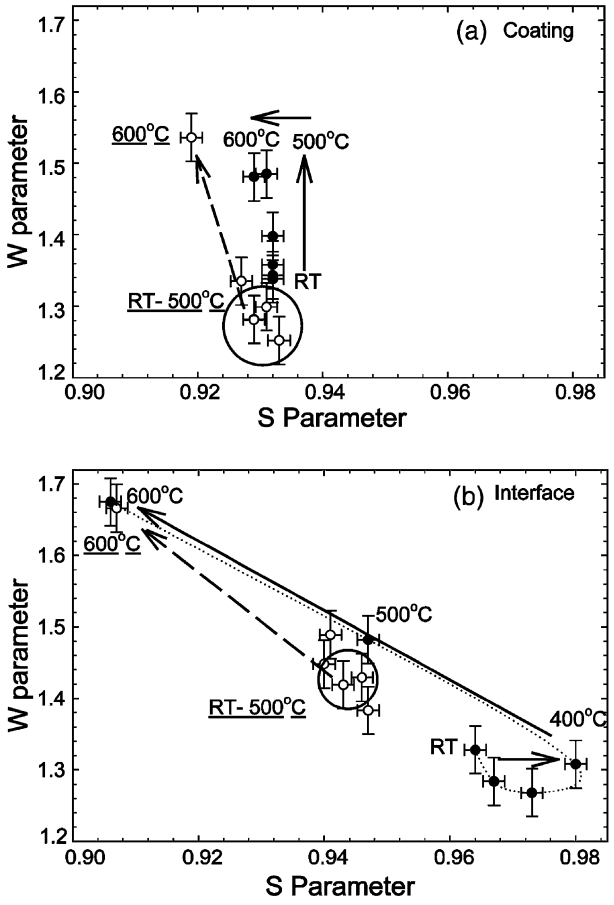

Fig. 4. *S*–*W* maps showing the CPs ascribed to positron annihilation as a function of annealing temperature, (a) inside the coating and (b) at the interface (the control samples 1—no N_2, is represented by open circles and 2—with N_2, is represented by closed circles). Both maps are plotted using the same scale in order to compare the changes observed.

CP indicating delamination of the film. There is a more gradual change for the sample containing N_2 (sample 2). Inside the coating the *W* parameter increases after annealing at 500 °C indicating a structural change in the layer due to release of hydrogen and further graphitisation as deduced from Raman spectroscopy experiments [19]. The open porosity, already present at the interface of the as deposited sample, becomes larger as the *S* parameter gradually increases with a constant *W* (no structural change) until 400 °C is reached (Fig. 5). This observation corresponds to the removal of physisorbed hydrogen from interfacial pores [23]. So it is important to note that positrons distinguish a large open porosity (related to an increase in *S*) of a delaminated interface (related to changes in the value of *S* and *W* towards surface values). However, according to Raman experiments [19], at approximately 400 °C the gas released during annealing is not only the release of 'unbound' hydrogen, but also the H bonded at tetrahedral sites to C. The growth of the sp^2 clusters, as seen

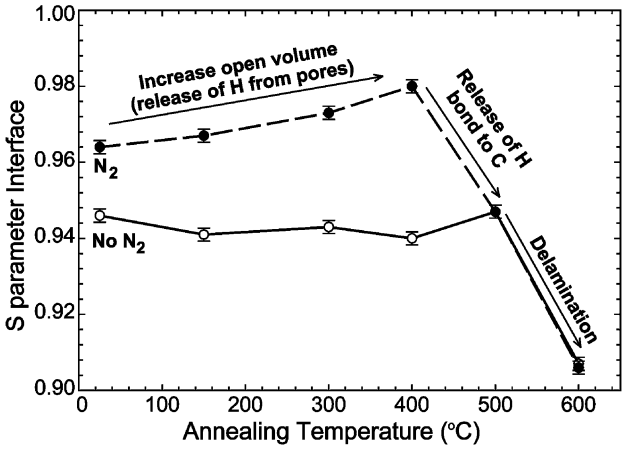

Fig. 5. The *S* parameter corresponding to the interface of the control samples 1 (no N_2, open circles) and 2 (N_2, closed circles) is plotted as a function of annealing temperature. The label RT denotes the samples prior to the annealing process.

by Raman spectroscopy, was also monitored by positrons showing a decrease in the value of *S* at 500 °C and an increase in the value of *W* at the interface. Finally at 600 °C the same *S*–*W* CP is reached as for sample 1 and 3 at 600 °C, and delaminated sample 4 before the annealing process (RT stands for room temperature in Fig. 4).

4. Conclusions

PBA has been performed on PVD hydrogenated amorphous carbon thin films synthesized under different deposition conditions. Delamination was observed after deposition in one of the samples studied. Annealing in vacuum up to 600 °C provokes the appearance of the first stages of delamination in the rest of the coatings. This was monitored by changes in the interfacial positron annihilation site. The role of nitrogen inclusion in the coating was followed through the study of two control samples deposited under the same conditions except for the inclusion of nitrogen in one case. The interface of the nitrogen-containing sample has a more open structure or pores. These pores are decorated with physisorbed hydrogen, whose release was monitored by positrons after annealing the sample up to 400 °C. Further annealing of the sample at 500 °C causes a restructuring both at the interface and in the coating due to release of bonded hydrogen and further graphitisation. The sample without nitrogen did not change noticeably during the annealing procedure until 500 °C. At 600 °C both samples showed the occurrence of delamination.

Acknowledgments

The authors thank the Foundation for Fundamental Research on Matter (FOM) and the Dutch Technology

Foundation STW (project number GTF.4901), for their financial and technical support.

References

[1] J. Robertson, Surf. Coat. Technol. 50 (1992) 185–203.
[2] Q. Wei, J. Narayan, Int. Mater. Rev. 45 (2000) 133–164.
[3] Q. Wei, J. Sankar, J. Narayan, Surf. Coat. Technol. 146–147 (2001) 250–257.
[4] A.M. Baranov, A.E. Varfolomeev, A.A. Nefedov, et al., Diamond Relat. Mater. 9 (2000) 649–653.
[5] F.M. Kimock, B.J. Knapp, Surf. Coat. Technol. 56 (1993) 273–279.
[6] J. Robertson, Tribol. Int. 36 (2003) 211–228.
[7] V.M. Tiainen, Diamond Relat. Mater. 10 (2001) 153–160.
[8] M. Brizuela, L.A. García, J.L. Viviente, I. Braceras, J.I. Onate, J. Mater. Sci. Mater. Med. 13 (2002) 1129–1133.
[9] J. Robertson, Mater. Sci. Eng. R 37 (2002) 129–281.
[10] M. Wittmer, D. Ugolini, J. Eitle, P. Oelhafen, Appl. Phys. A 48 (1989) 559–566.
[11] Y.H. Cheng, Y.P. Wu, J.G. Chen, X.L. Qiao, C.S. Xie, Diamond Relat. Mater. 8 (1999) 1214–1219.
[12] S.R.P. Silva, J. Robertson, G.A.J. Amaratunga, et al., J. Appl. Phys. 81 (1997) 2626–2634.
[13] P. Wood, T. Wydeven, O. Ysuji, Thin Solid Films 258 (1995) 151–158.
[14] D.F. Franceschini, C.A. Machete, F.L. Freire Jr., Appl. Phys. Lett. 60 (1992) 3229–3231.
[15] A. van Veen, H. Schut, P.E. Mijnarends, in: P. Coleman (Ed.), Positron Beams and their Applications, World Scientific Publishing Co, 2000, Chapter 6.
[16] D.T. Britton, M. Härting, M. Hempel, D. Gxawu, K. Uhlman, Appl. Surf. Sci. 149 (1999) 130–134.
[17] F. Rossi, B. André, A. van Veen, et al., J. Phys. III 5 (1995) C1 179–C1 191.
[18] L.G. Jacobsohn, G. Capote, M.E.H. Maia da Costa, D.F. Franceschini, F.L. Freire Jr., Diamond Relat. Mater. 11 (2002) 1946–1951.
[19] F. Rabbani, R. Escobar Galindo, W.M. Arnoldbik, S. van der Zwaag, A. van Veen, H. Schut, Diamond Relat. Mater., submitted for publication.
[20] A. van Veen, J. Trace Microprobe Tech. 8 (1990) 1–29.
[21] A. van Veen, H. Schut, J. de Vries, R.A. Hakvoort, M.R. Ijpma, in: P.J. Schultz, G.R. Massoumi, P.J. Simpson (Eds.), AIP 218, Positron Beams for Solids and surfaces, 1990, pp. 171–196.
[22] J.P. Holgado, R. Escobar Galindo, A. van Veen, H. Schut, J.Th.M. de Hosson, A.R. González-Elipe, Nucl. Instrum. Meth. B 194 (2002) 333–345.
[23] F. Rabbani, B.M. Vogelaar, Diamond Relat. Mater., accepted for publication.